J Fluoresc (2014) 24:1379–1387
DOI 10.1007/s10895-014-1400-5

ORIGINAL PAPER

Photoinduced Intramolecular Electron Transfer and Electronic Coupling Interactions in π- Expanded Imidazole Derivatives

J. Jayabharathi · V. Kalaiarasi · V. Thanikachalam · K. Vimal

Received: 23 January 2014 / Accepted: 23 April 2014 / Published online: 20 June 2014

Abstract An intramolecular excited charge transfer (CT) analysis of imidazole derivatives has been made. The determined electronic transition dipole moments has been used to estimate the electronic coupling interactions between the excited charge transfer singlet state (^{1}CT) and the ground state (S_0) or the locally excited state (^{1}LE). The properties of excited ^{1}CT state imidazole derivatives have been exploited by the significant contribution of the electronic coupling interactions. The excited state intramolecular proton transfer (ESIPT) analysis has also been discussed.

Keywords Charge transfer · Donor- acceptor · Electronic coupling · ESIPT

Introduction

The analysis of the charge transfer (CT) absorption (^{1}CT←S_0), radiative and radiationless charge recombination (CR) processes (^{1}CT→S_0) have been explained by photoinduced electron transfer (ET) processes [1–5]. Mulliken and Murrell models of molecular CT complexes leads to the determination of rate of radiative ET processes [6–8] and also to the molecular conformation of the states involved in the excited-state ET process [9–13]. The relatively large values of the electronic transition dipole moments (M_{flu}) of CT fluorescence indicate a non orthogonal geometry of the donor (D) and acceptor (A) subunits in the lowest excited ^{1}CT states. The 9-anthryl and 9-acridyl derivatives of aromatic amine show the dependence of electronic structure and conformation of fluorescent ^{1}CT state on solvation [14, 15]. In low polar environment the interactions between ^{1}CT state and locally excited (LE) states lead to a more planar conformation of D and A moieties than that in the ground state. In more polar solvents the relatively strong solute solvent interactions prevent the flattening of the excited D-A system and its conformation is similar to that in the ground state. Proton- and charge-transfer reactions are the most fundamental processes involved in chemical reactions as well as in living systems [16, 17]. Among the various studies of proton transfer, organic molecules exhibiting excited state intramolecular proton transfer (ESIPT) have attracted considerable research interest from the viewpoint of the development of new functional materials for optoelectronic applications such as UV photo stabilizers [18], photo switches [19], fluorescent probes [20] and organic light-emitting diodes (OLEDs) [21]. Photoinduced ESIPT is generally observed for organic compounds featuring both a protic acid group (e.g., OH, NH_2, $NHSO_2R$, etc.) and a basic site (N-, C=O, etc.) with a suitable conformation, one that forms an intramolecular hydrogen bond within the distance of 2.0 Å. In this article, we report the synthesis, characterisation and solvatochromism of newly synthesized π-expanded imidazole derivatives. The influence of solvents on the photophysical properties of the imidazole derivatives with solvent polarity function have been discussed in terms of absorption, emission, dipole moments, radiative and non-radiative rate constants change in free energy and reorganisation energy.

Experimental

Spectral Measurements

The proton and proton decoupled ^{13}C NMR spectra were recorded using a Bruker 400 MHz NMR spectrometer (Bruker biospin, California, USA) operating at 400 and 100 MHz, respectively. The mass spectra of the samples were obtained using a Thermo Fischer LC-Mass spectrometer in FAB mode.

J. Jayabharathi (✉) · V. Kalaiarasi · V. Thanikachalam · K. Vimal
Department of Chemistry, Annamalai University,
Annamalainagar 608002, Tamilnadu, India
e-mail: jtchalam2005@yahoo.co.in

The UV–vis absorption and fluorescence spectra were recorded with PerkinElmer Lambda 35 spectrophotometer and PerkinElmer LS55 spectrofluorimeter, respectively. Lifetime measurements were carried out with a nanosecond time correlated single photon counting (TCSPC) spectrometer Horiba Fluorocube-01-NL lifetime system with Nano LED (pulsed diode exCitation source) as the excitation source and TBX-PS as detector. The fluorescence decay was analyzed using DAS6 software. The quantum yield was measured in dichloromethane using coumarin 47 in ethanol as the standard [22–24].

Solvatochromic Comparison Method (SCM)

The individual contribution of different solvent effects have been analysed by a solvatochromic comparison method (SCM) [25]. The equation using dielectric effect of solvents (π^*), hydrogen-bond donor ability (α) and hydrogen-bond acceptor ability (β) of the solvents on the spectral properties,

$$E = E^0 + c\pi^* + aa + b\beta \quad (1)$$

where, a, b, and c are the coefficients and E^0 is the spectral maxima independent of solvent effects. The values of π^*, α and β of different solvents have been taken from Kamlet et al. parameters [25].

Computational Details

The quantum chemical calculations were carried out using the Gaussian 03 [26] package. Optimization and HOMO—LUMO frontier orbital of imidazole derivatives were performed using density functional theory (DFT) and also time-dependent DFT (TD-DFT) using B3LYP/6-31G (d,p) basis set, respectively.

Synthesis of 1-(naphthalene-1-yl) -2,4,5-triphenyl-1H-imidazole (1)

A mixture of benzil (10 mmol), α-napthylamine (10 mmol), benzaldehyde (10 mmol) and ammonium acetate (10 mmol) in ethanol was refluxed at 80ºC. The reaction was monitored by thin layer chromatography and the product, 1-(naphthalene-1-yl)-2,4,5-triphenyl-1H-imidazole was purified by column chromatography [27–29] using benzene-ethyl acetate (9:1) as the eluent. M.p. 251ºC, Anal. calcd. for $C_{31}H_{22}N_2$: C, 88.12; H, 5.25; N, 6.63; Found: C, 86.89; H, 4.02; N, 5.35. ^{1}H NMR (400 MHz, $CDCl_3$): δ, 7.92 (d, J=6.8 Hz, 3H), 7.56 (d, J=6.4 Hz, 6H), 7.43 (t, 3H), 7.26–7.37 (m, 10H). ^{13}C NMR (100 MHz, $CDCl_3$ and DMSO): δ 125.68, 127.10, 128.11, 128.27, 128.33, 128.48, 130.01, 132.92, 146.13. MS: m/z 422 [M^+].

Synthesis of 2-(1-(naphthalene-1-yl) -4,5-diphenyl-1H-imidazole-2-yl)aniline (2)

A mixture of benzil (10 mmol), α-napthylamine (10 mmol), *o*-nitrobenzaldehyde (10 mmol) and ammonium acetate (10 mmol) in ethanol was refluxed at 80ºC. The reaction was monitored by thin layer chromatography and the product, 1-(naphthalene-1-yl)-2-(2-nitrophenyl)-4,5-diphenyl-1Himidazole was purified by column chromatography using benzene-ethyl acetate (9:1) as the eluent. Recrystallization from ethyl acetate yielded a yellow crystalline solid. The 1-(naphthalene-1-yl)-2-(2-nitrophenyl)-4,5-diphenyl-1H-imidazole (3.5 mmol) was dissolved in 15 ml of ethanol-ethylacetate and reduced using Sn/HCl catalyst. The catalyst was filtered off and the solvent was evaporated. The formed amino product was crystallised from ethylacetate. M.p. 254ºC, Anal. calcd. for $C_{31}H_{23}N_3$: C, 85.10; H, 5.30; N, 9.60; Found: C, 85.09; H, 5.25; N, 9.56. ^{1}H NMR (400 MHz, DMSO): δ, 7.92 (d, J=5.2 Hz, 3H), 7.56 (d, J= 3.2 Hz, 6H), 7.43 (t, 3H), 7.26–7.37 (m, 10H), 11.62 (s, 1H). ^{13}C NMR (100 MHz, DMSO): δ 125.71, 127.28, 128.32, 128.34, 128.43, 129.51, 130.09, 132.97, 146.15. MS: m/z 437 [M^+].

Synthesis of 4-Methyl-N-(2-(1-naphthalen-1-yl) -4,5-diphenyl-1H-imidazole-2yl)phenylbenzene sulfonamide (3)

P- Toluene sulphonyl chloride (0.7 mmol) was added to a solution of 2-(1-(naphthalene-1-yl)-4,5-diphenyl-1H-imidazole-2-yl)aniline **2** (0.5 mmol) in pyridine (4 ml) and the mixture was heated to reflux for 3 days. The reaction mixture was poured into ice and the formed product was purified by column chromatography using benzene-ethylacetate (9:1) as the eluent. Recrystallization from ethyl acetate solution yielded a white crystalline solid. M.p. 262ºC, Anal. calcd. for $C_{38}H_{29}N_3O_2S$: C, 77.13; H, 4.94; N, 7.10; O,5.41; S, 5.42;. Found: C, 77.08; H, 4.89; N, 7.03; O, 5.38; S, 5.40; ^{1}H NMR (400 MHz, DMSO): δ, 2.34 (s, 3H), 6.10 (bs, 2H), 7.93 (d, J=3.2 Hz, 3H), 7.56 (d, J=6 Hz, 6H), 7.43 (t, 4H), 7.27–7.37 (m, 10H), 12.03 (s, 1H). ^{13}C NMR (100 MHz, DMSO):δ 21.31, 125.72, 127.18, 128.31, 128.39, 128.42, 128.51, 130.09, 132.96, 136.32, 145.21, 146.23. MS: m/z 591 [M^+].

Results and Discussion

Electronic Spectral Analysis

Solvent effects on absorption and fluorescence spectra of the D–A derivatives of imidazole are presented in Fig. 1. The absorption spectrum in n-hexane shows a shoulder with a

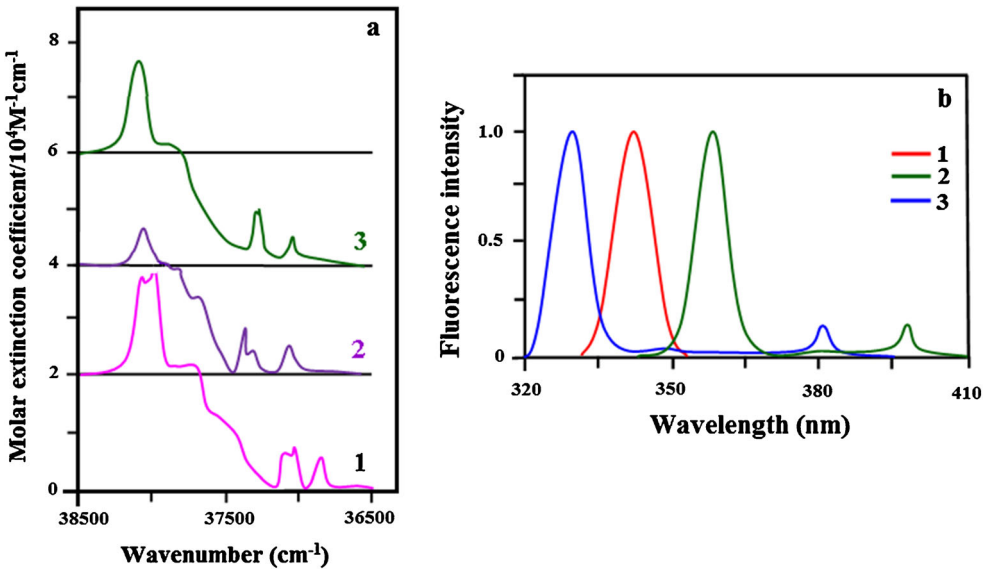

Fig. 1 **a** Room temperature absorption spectra of imidazoles **1**–**3**; **b** Room temperature emission spectra of **1**–**3** in dioxane

maximum between 37,037 and 37,174 cm^{-1} and a dominant band around 38,022 cm^{-1}. The nonorthagonal geometry of similar imidazole derivatives are recently reported by our research group [27–29]. The two low lying in plane polarized transition are assigned as $^1(\pi, \pi^*) \leftarrow S_0$ transition localized mainly in the donar subunit corresponds to the plats notation ^1L_b and ^1L_a excited states [30, 31] and the lowest out-of-plane polarized transitions are assigned as $^1CT \leftarrow S_0$ transitions. The TD-DFT theoretical calculations predict a non-planar conformation with the torsional angle ($_{A–D}$) between the D and A subunits as 44.3° (**1**), 51.2° (**2**) and 65.3° (**3**), respectively (Fig. 2a). The transition $^1L_a \leftarrow S_0$ carries relatively high oscillator strength (*f*). According to these calculations, the increase of the $_{A–D}$ value leads to lowering of spectral position and of *f* value of latter transition (Table 1). The absorption data have been analyzed using the solvent comparison method and the coefficients are tabulated (Table 2). The representative equation obtained from this approach for compound **3** is,

$$E(cm^{-1}) = 37615 - 18296\pi^* + 3974\alpha - 26510\beta \quad (2)$$

Negative values of π^* and β indicate that these two parameters contribute to the stabilisation of ground state.

The emission spectra of the studied imidazole derivatives show a red shift from hexane to water. The fluorescence band is structured in a nonpolar solvent. Therefore, emission can be originated from the LE state in a nonpolar solvent. However, in polar aprotic and polar protic solvents broad structureless bands are noticed. There is a progressive significant bathochromic shift on increasing the polarity of the solvent, characteristics of a chargetransfer (CT) emission [30]. The progressive bathochromic shift of charge-transfer band on increasing the polarity of the solvent depicts that the fluorescence originates from a highly polar state. The relative intensity of low energy emission of compounds increases with increasing polarity of the medium [30–32]. The CT emission is dominant in polar solvents, the red shifted emission and increase of Stokes shift with increasing solvent polarity point to the CT character of fluorescent states. A large contribution of inner reorganization energy influences the CT fluorescence [2, 3, 5, 33, 34]. The effect of solvent polarity on the fluorescence maximum is more intense than that on the absorption maximum so that the

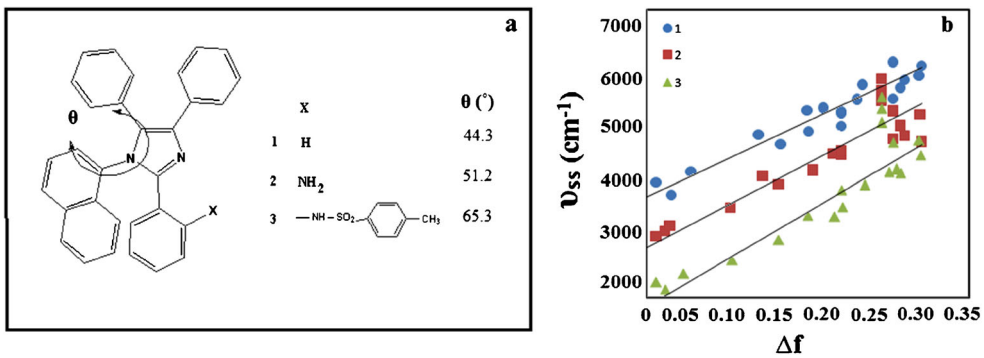

Fig. 2 **a** The torsional angle ($_{A–D}$) for imidazole derivatives. **b** Lippert—Mataga plot of Stokes shift against solvent polarity function (Δf) of all solvents

Table 1 Comparison between TD-DFT/B3LYP/6-31G(d,p) calculated energies (**ΔE**) and oscillator strength (*f*) corresponding to the transitions ^{1}(n, π*), ^1L_b and ^1L_a excited states and experimental energies (ΔE) for **1-3**

Compound	Transition	TD-DFT B3LYP/6-31G(d,p)		Experimental ΔE/10^3 cm^{-1}
		ΔE/10^3 cm^{-1}	*f*	
1	^{1}(n,π*)	37.40	0.0132	36.98
	^1L_b	38.20	0.0045	37.82
	^1L_a	39.85	0.2985	39.12
2	^{1}(n,π*)	32.19	0.0105	31.89
	^1L_b	35.46	0.0164	35.12
	^1L_a	38.15	0.1654	37.92
3	^{1}(n,π*)	31.26	0.0112	30.85
	^1L_b	34.65	0.0156	34.10
	^1L_a	37.82	0.0942	37.01

emitting state is more polar than the ground state [35–37]. The emission yields are more prominent in polar solvents compared to that of non polar solvents. The behaviour of imidazole derivatives with solvent polarities may be interpreted in terms of difference in ground and excited states dipole moments [$\Delta\mu=\mu_e-\mu_g$]. Solvatochromic effect can be studied using Lippert–Mataga equation [38],

$$\overline{\overline{\nu}}_{ss} = \left[2\left(\mu_e-\mu_g\right)/\mathrm{hca}^3\right]\Delta f + \nu_{SS^\circ} \quad (3)$$

where $\overline{\nu}_{SS}$ is the Stokes shift, the superscript o indicates the absence of solvent, μ_g and μ_e are ground and excited states dipole moments, respectively, h is Planck's constant, c is velocity of light and a is Onsager cavity radius. The orientation polarizability (Δf) is,

$$\Delta f = [(\varepsilon-1)/(2\varepsilon+1)-\left[\left(n^2-1\right)/\left(2n^2+1\right)\right]$$

where ε and n are solvent dielectric constant and refractive index, respectively and the Lippert-Mataga plot is linear as shown in Fig. 2b. A good linear variation [39] is also obtained between the emission wavenumber and E_T (30) as shown in Fig. 3a. Ground state dipole moment μ_g of these imidazole derivatives are calculated theoretically using Gaussian-03 [26]. Using μ_g values [3.13D (**1**), 3.56D (**2**) and 6.95D (**3**)] and the slope of Lippert–Mataga plot, the calculated μ_e is in the range of 14.0–25.7 D for the studied imidazoles. SCM has also been applied to analyze the fluorescence data and the coefficient values are displayed in Table 2. which results The representative equation for compound **3** is

$$E\left(\mathrm{cm}^{-1}\right) = 38732–17020\pi^* + 35091\alpha−22856\beta \quad (4)$$

This equation shows that the parameters π^* and β contribute to the stabilization of excited state [40]. The calculated ratio of β over π* [0.52(υ_{abs}) & 1.12 (υ_{emi}) (**1**), 1.68(υ_{abs}) & 0.61(υ_{emi}) (**2**), and 1.44(υ_{abs}) & 1.34(υ_{emi}) (**3**)] reveal that interactions between imidazole derivatives and solvents with basicity property (β) predominate in the excited state. The solvatochromic effects on the spectral position of the CT absorption can be given by,

$$\mathrm{hc}\widetilde{\mathrm{U}}_{\mathrm{abs}} \approx \boldsymbol{hc}\widetilde{\mathrm{U}}^{vac}_{\mathbf{abs}} - 2\mu_g\left(\mu_e-\mu_g\right)/\left[(\varepsilon-1/2\,\varepsilon+1)-\tfrac{1}{2}\left(n^2-1/2n^2+1\right)\right] \quad (5)$$

where μ_g and μ_e are the dipole moment of the solute in ground and excited states, respectively, ν_{abs} and $\nu^{vac}_{\mathbf{abs}}$ are the spectral

Table 2 Adjusted coefficients ($(\upsilon_x)_0$, c_a, c_b and c_c) for the multilinear regression analysis of the absorption (υ_{ab}) and fluorescence (υ_{fl}) wavenumbers and Stokes Shift ($\Delta\upsilon_{ss}$) of imidazole derivatives (**1**–**3**) with solvent polarity/polarizability, acid and base capacity using the Kamlet scales

	(υ_x)	$(\upsilon_x)_0$ cm^{-1}	(π*)	c_α	c_β
1	υ_{ab}	(4.07±0.06)×10^4	(3.06±1.60)×10^3	−(0.27±0.04)×10^3	−(1.61±0.53)×10^3
	υ_{fl}	(2.51±0.06)×10^4	−(13.53±2.32)×10^3	(24.66±3.60)×10^3	−(15.26±2.84)×10^3
	$\Delta\upsilon_{ss}$	(1.55±0.12)×10^4	(16.60±3.84)×10^3	−(24.93±5.55)×10^3	(13.65±1.26)×10^3
2	υ_{ab}	(3.82±0.06)×10^4	(2.53±0.83)×10^3	(3.18±1.07)×10^3	−(4.263±2.64)×10^3
	υ_{fl}	(2.61±0.09)×10^4	−(16.91±2.82)×10^3	(27.95±4.77)×10^3	−(16.11±3.92)×10^3
	$\Delta\upsilon_{ss}$	(1.20±0.12)×10^4	(19.45±3.82)×10^3	−(24.76±2.48)×10^3	(11.84±2.20)×10^3
3	υ_{ab}	(3.76±0.07)×10^4	(18.29±3.93)×10^3	(39.74±4.66)×10^3	−(26.51±1.80)×10^3
	υ_{fl}	(3.87±0.07)×10^4	−(17.02±4.30)×10^3	(35.09±5.68)×10^3	−(22.85±3.25)×10^3
	$\Delta\upsilon_{ss}$	(0.88±0.14)×10^4	(35.31±3.03)×10^3	−(74.84±6.72)×10^3	(49.36±3.56)×10^3

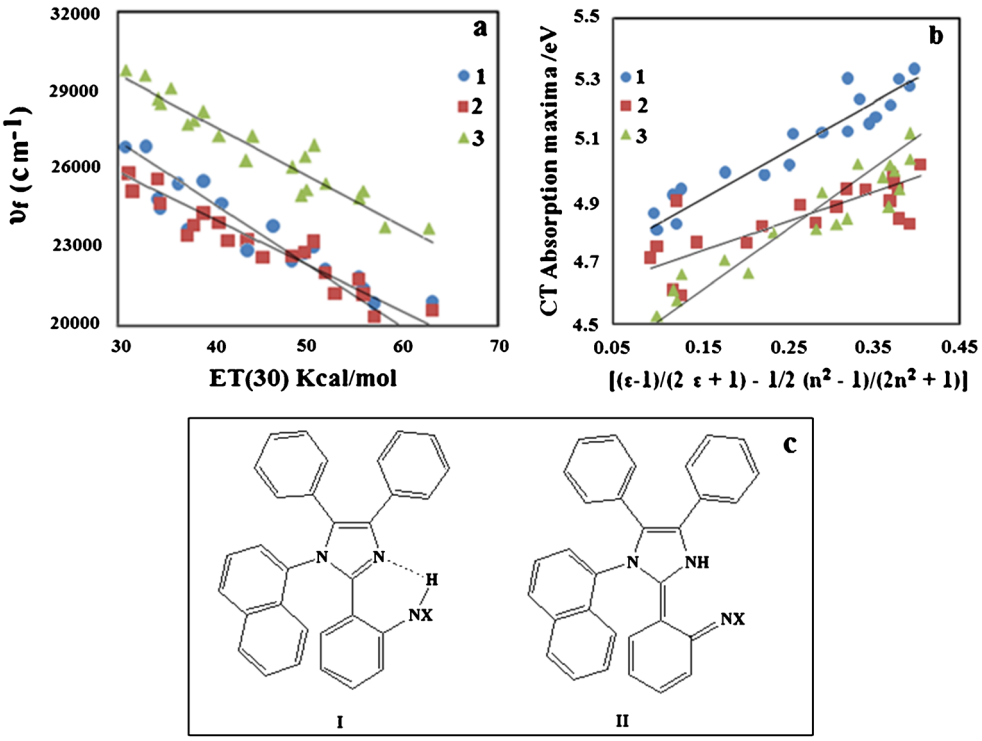

Fig. 3 **a** Plot of fluorescence maxima in terms of wave number (cm-1) and E_T (30) values; **b** Solvatochromic effects on the spectral position of the CT absorption maxima; **c** Isomeric forms (I&II) of amino imidazole derivatives

positions of a solvent equilibrated absorption maxima and the value extrapolated to the gas phase, respectively [41, 42]. From the linear plot (Fig. 3b) of energy $hc\overline{\upsilon}_{abs}$ versus solvent polarity function f (ε, n), the values of μ_g $(\mu_e-\mu_g)/a_o^3$ have been calculated and the same is displayed in Table 3. The observed red shifted spectral position and increase of Stokes shift with increasing solvent polarity point to the CT character of the fluorescent states indicate the absolute values of μ_e are much higher than those of μ_g. Since the molecules in the excited state stays sufficiently long time with respect to the orientation relaxation time of the solvent [43–47], the excited state dipole moment μ_e can also be estimated by the fluorescence solvatochromic shift method. The solvatochromic effects on the spectral position of the CT emission can be given by [43–47],

$$hc\widetilde{U}_{flu}{}^{CT} \approx hc\widetilde{U}_{flu}^{vac} - 2\,\mu_e\left(\mu_e-\mu_g\right)/a_0^3\left[(\varepsilon-1/2\,\varepsilon+1)-\tfrac{1}{2}\left(n^2-1/2n^2+1\right)\right] \quad (6)$$

where $hc\widetilde{U}_{flu}^{CT}$ and $hc\widetilde{U}_{flu}^{vac}$ are the energies corresponding to the spectral position of the CT fluorescence maxima in solution and to the values extrapolated to the gas phase, respectively. From the linear plot of energy $hc\widetilde{U}_{flu}^{CT}$ against solvent polarity function f (ε, n), the values of μ_e $(\mu_e-\mu_g)/a_o^3$ have been calculated as 2.01 eV (**1**), 2.79 eV (**2**), and 2.05 eV (**3**) (Table 3). A significant deviation from the linearity may due to strong interactions between the lowest ^{1}CT state and a closely lying excited state of different nature. The radiationless (k_{nr}) and radiative (k_r) rate constants are related to the CT emission quantum yield (Φ) and lifetime (τ) as shown in the equation, $k_{nr}=1/(\tau)-\Phi/(\tau)$; $k_r=\Phi/\tau$ [48, 49]. The higher radiationless deactivation (k_{nr}) of the studied compounds is probably due to a fast internal conversion (IC) to the ground state or an intersystem crossing (ISC) to a close lying triplet state (Table 3).

Table 3 Determination of dipole moments from the slopes of the Solvatochromic Plots and Solvent effects on the spectral position of CT fluorescence maxima (υ_f, cm^{-1}), quantum yields (ϕ), decay time (τ, ns), radiative (k_r, 10^8 s^{-1}), non radiative (k_{nr}, 10^8 s^{-1}) rate constants and electronic transition dipole moments ($M_{flu,\,D}$) for the imidazole derivatives

Compound	μ_g $(\mu_e-\mu_g)/a_0{}^3$ (eV)			μ_e $(\mu_e-\mu_g)/a_0{}^3$ (eV)		$(\mu_e-\mu_g)^2/a_0{}^3$ (eV)	
1	1.67			2.01		1.41	
2	1.87			2.79		1.65	
3	1.92			2.05		1.99	
	Solvent	υ_f	ϕ	τ	k_r	k_{nr}	M_{flu}
1	Cyclohexane	38,759	0.49	1.3	3.76	3.92	3.8
	Benzene	39,840	0.40	1.4	2.86	4.28	4.2
	Tetrahydrofuran	40,650	0.35	1.6	2.19	4.06	4.0
	Acetonitrile	42,553	0.39	1.6	2.44	3.81	3.4

Under the assumption that the CT fluorescence corresponds to the state reached directly upon excitation, the quantity $(\mu_e-\mu_g)^2/a_o^3$ can be evaluated from the solvation effect on Stokes shift,

$$hc\left(\widetilde{U}_{abs}-\widetilde{U}_{flu}\right)=hc\left(\mathbf{h}c\widetilde{U}_{\mathbf{abs}}^{vac}-\mathbf{h}c\widetilde{U}_{flu}^{vac}\right)+2\left(\mu_e-\mu_g\right)^2/a_0^3\left[(\varepsilon-1/2\varepsilon+1)-1/2\left(n^2-1/2n^2+1\right)\right] \quad (7)$$

The compounds studied show a linear correlation between the energy $hc_{abs}-hc_{flu}$ and the solvent polarity function f (ε, n) in a polar environment and also in all the solvents studied. With the assumption $\mu_e >> \mu_g$ and with the effective spherical radius (a_0) of the molecules as 6.03 Å (**1**), 6.11 Å (**2**) and 6.73 Å (**3**), the molecular dimension of the compounds calculated by molecular mechanics, the calculated μ_e are 14.23 D (**1**), 20.09 D (**2**) and 25.68 D (**3**) for the studied molecules. The large values of $\Delta\mu=\mu_e-\mu_g\approx$11.10 D (**1**), 16.53 D (**2**) and 18.73 D (**3**) corresponds to a charge separation of about 0.3–0.4 nm which roughly agrees with centre-to-centre distance between the donor and acceptor moieties of the compounds.

A dual fluorescence detected for 2-(1-(naphthalene-1-yl)-4,5-diphenyl-1H-imidazole-2-yl)aniline (**2**) with emission peaks centered at 368 and 405 nm. The strong emission at 368 nm is assigned to intramolecular hydrogen bonded amino form I and the weak emission at 405 nm interpreted with the presence of the imine form II (Fig. 3c). The absence of additional peak at longer wavelength confirms the absence of intramolecular hydrogen bond in compound **1**. It is evident that intramolecular hydrogen bonding is the driving force for ESIPT and the dual fluorescence behaviour of 1-(naphthalene-1-yl)-2,4,5-triphenyl-1H-imidazole. For better understanding the ESIPT mechanism in 2-(1-(Naphthalene-1-yl)-4,5-diphenyl-1H-imidazole-2-yl)aniline, DFT calculation have been performed to know the electron density of its isomers I and II in ground and excited states. In the excited state the imidazole nitrogen atom (−0.39 au) becomes richer in electrons than the amino nitrogen atom (−0.25 au) and causes the intramolecular proton transfer from the amino group to the imidazole nitrogen atom. The potential energy surface (PES) curves for the interconversion of isomers I and II of 2-(1-(naphthalene-1-yl)-4,5-diphenyl-1H-imidazole-2-yl)aniline in the ground state for isolated molecule is 7.2 kcal/mol and that in ethanol is 4.1 kcal/mol. The corresponding value in the excited state for the isolated molecule is 14.9 and that in ethanol is 9.3 kcal/mol, respectively. The barrier for interconversion in the excited state is much higher than that in the ground state which confirms in ground state, these two isomers are interconvertible. Similar trend was observed for compound 4-methyl-N-(2-(1-naphthalen-1-yl)-4,5-diphenyl-1H-imidazole-2yl)phenyl)benzene sulfonamide **(3)**. The introduction of electron withdrawing tosyl group reduces the electron density around nitrogen atom, and makes the easy viability of ESIPT process.

The wavefunction of ^{1}CT state [49] is a linear combination of zero-order ET state (^{1}ET) with various locally excited $^1(\pi, \pi^*)$ states and with the ground state (S_0),

$$\Psi_{CT}^1 \cong C_{ET}\phi_{ET}^1 + C_a\phi_{La}^1 + C_b\phi_{Lb}^1 + C_0\phi_{s0}^1 \quad (8)$$

where $\phi_{s0}^1, \phi_{ET}^1, \phi_{La}^1$, and ϕ_{Lb}^1 represent the closed shell configuration of the ground state, the zero order wave functions of the pure ^{1}ET state (ET from the occupied HOMO orbital of the donor to the vacant LUMO orbital of the acceptor) and the ^1L_a and ^1L_b states of the donor moieties, respectively. The frontier molecular orbital diagram (Fig. 4a) shows that the HOMO electron density is localised on the imidazole moiety and the LUMO electron density is localised on the naphthyl moiety. Additionally, looking at the computed molecular orbitals of **1**–**3,** there is a clear charge transfer from the HOMO to the LUMO orbitals. The values of Δμ suggest that the wave function of the ^{1}CT states are in the order **3>2>1** which is in agreement with the value of energy $hc\widetilde{U}_{flu}^{vac}$ **[3>2>1]**. Therefore the contribution of the $^1(\pi, \pi^*)$ character to the wavefunction should decrease in the order, **3>2>1**.

The electronic transition dipole moments (M_{flu}) is depend upon the radiative (k_f) rate constant as shown in the following equation [7–9, 49–57],

$$k_f = \frac{64\pi 4}{3h}\left(\widetilde{n_{flu}^{\upsilon}}vCT\right)^3|M_{flu}|^2 \quad (9)$$

The M_{flu} values can be approximated by a Mulliken model [7, 53],

$$M_{flu}\approx V_0\left(\mu_e-\mu_g\right)/\mathbf{h}c\widetilde{U}_{\mathbf{flu}}^{vCT} \quad (10)$$

With $\Delta\mu=\mu_e-\mu_g\approx$11.10 D (**1**), 16.53 D (**2**) and 18.73 D (**3**), the calculated electronic coupling element V_0 between the ^{1}CT state and the ground state, values are 0.19 eV (**1**), 0.21 eV(**2**) and 0.25 eV(**3**). The electronic coupling element V_0, values are determined by the interactions between the atoms forming the A–D bond, and theoretically predicted by Dogonadze et al. [57] method.

$$V_0 = C_{\mathbf{LUMO}}^A C_{\mathbf{HOMO}}^D \beta_{AD}\cos(\theta_{A-D}) + \text{const.}, \quad (11)$$

where $C_{\mathbf{LUMO}}^A$ and $C_{\mathbf{HOMO}}^D$ are the LCAO coefficients of the atomic orbitals located on the atoms which form the A–D bond of the lowest unoccupied molecular orbital (LUMO) and of the

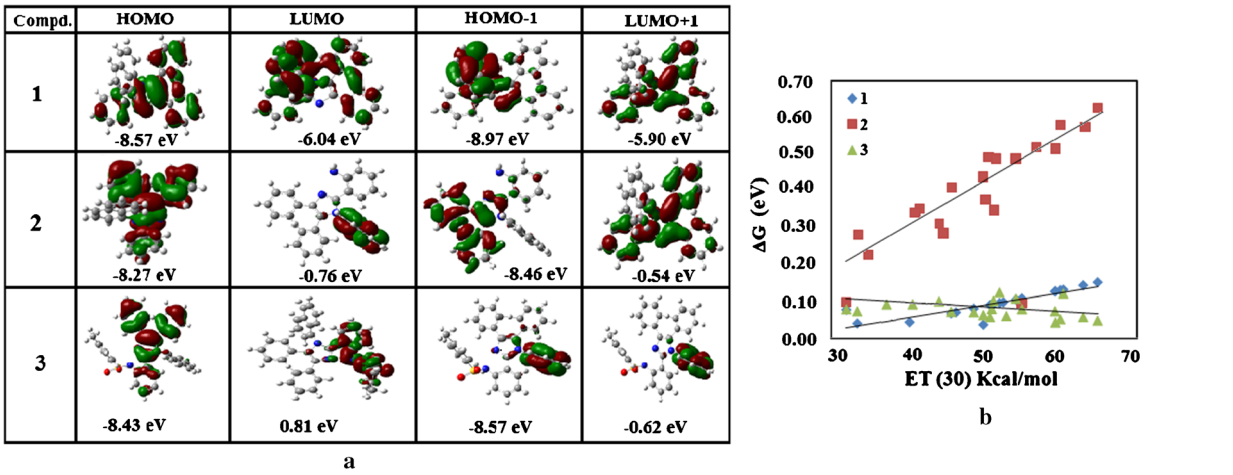

Fig. 4 **a** Computed HOMO-LUMO orbitals contour map **b** Plot of ΔG_{solv} versus $E_T(30)$

highest occupied molecular orbital (HOMO), respectively; The β_{AD} is the resonance integral for these atoms and constant is related to the electronic interactions between the pairs of atoms in the D–A molecule [58]. The values of $C^{A}_{\mathbf{LUMO}}$=0.58 and $C^{D}_{\mathbf{HOMO}}$ 0.79 were calculated by the DFT/B3LYP/6-31G (d,p) method. Assuming β_{AD} is 1.8 eV and the donar-acceptor twist angle $_{A\text{-}D}$ 44.3° (**1**), 51.2° (**2**) and 65.3° (**3**) the electronic coupling element V_0 is calculated which are in agreement with the experimental values obtained using Eq. 10.

The free energy changes of solvation and reorganization energies of **1**–**3** in various solvents have been estimated. According to Marcus [59, 60], E (A)=$\Delta G_{solv}+\lambda_1$ and E (F)=$\Delta G_{solv}-\lambda_0$, where E(A) and E(F) are absorption and fluorescence band maxima in cm^{-1}, respectively, ΔG_{solv} is the difference in free energy of the ground and excited states in a given solvent and λ represents the reorganization energy. Under the condition $\lambda_0 \approx \lambda_1 \approx \lambda$, we get, E (A)+E (F)=$2\Delta G_{solv}$; E (A)—E (F)=2 λ. The plot of ΔG_{solv} versus $E_T(30)$ has been shown in Fig. 4b. The mechanism of electronic coupling interaction between the donar and the acceptor through the intervening σ- bond has been discussed by Turro etal [60–62]. The rate constant k_{ET} for electron transfer has been calculated using the equation, $k_{ET}=(1/\tau)(\lambda_0/16\pi RT)^{1/2}\exp(-\lambda_0/4RT)$. The rate constant k_{ET} plotted against the change in free energy as shown in Fig. 5a. It is shown that both static (through λ_0) and dynamic (through τ) dielectric properties of the solvents may strongly influence the rate of electron transfer process. Inspection of the data reveal an initial rise of the rate with increasing free energy change followed by an inverted region where further increases of the driving force leads to a decrease in rate. The obtained free energy change [less than 0.69 eV] and the reorganisation energy [0.3–0.6 eV] indicate the electron transfer is in the inverted Marcus region [60–62]. The reorganisation energy (λ_0) is related to the low frequency motion such as reorientation of the solvent shell (λ_s) as well as any other low frequency and medium frequency nuclear motions of the solute ($\delta\lambda_0$). The solvatochromic effect on λ_0 is related by the following expression,

$$\lambda_{0\approx}\delta\lambda_{0+}\lambda_{s\approx}\delta\lambda_{0+}\left(\mu_e-\mu_g\right)^2/a_0^3\left[(\varepsilon-1/2\,\varepsilon+1)-\tfrac{1}{2}\left(n^2-1/2n^2+1\right)\right] \quad (12)$$

The values of $(\mu_e-\mu_g)^2/a_o^3$ [1.41 eV (**1**), 1.65 eV (**2**) and 1.99 eV (**3**)] obtained from the slope of the plot (Fig. 5b) supports again the wave function of the ^{1}CT state are of the order **3>2>1**.

Conclusions

Solvent induced transformation of electronic structure of ^{1}CT states of D–A derivatives of imidazoles has been analysed.

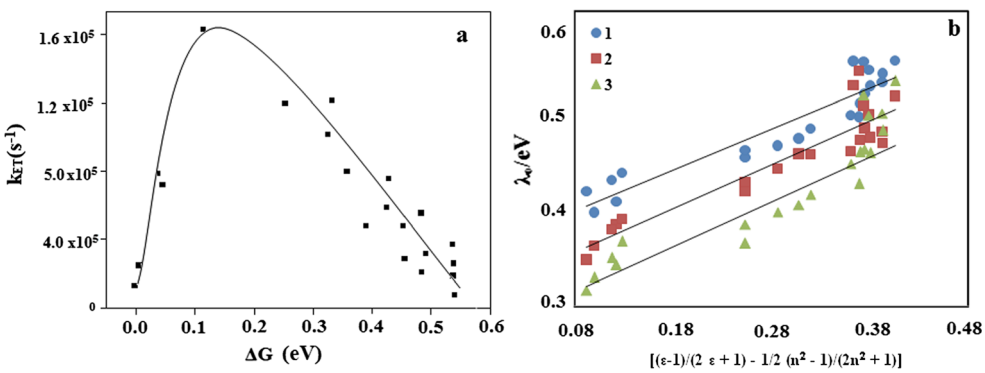

Fig. 5 **a** Rate constant k_{ET} plotted against the change in free energy. **b** Dependence of the reorganization energy λ_0 related to the low-frequency solvent and solute motions accompanying the excited-state electron transfer on the solvent polarity function

The dominant CT emission of the imidazole derivatives is most probably due to the excited state intramolecular ET. The electronic coupling element V_0 calculated by using $\Delta\mu$ gives an information that the conformation of the emitting ^{1}CT states does not differ notably from that in the ground state. The calculated free energy change and reorganisation energy indicate the electron transfer is in the inverted Marcus region. The viability of ESIPT process in amino imidazole derivatives have also been analysed.

Acknowledgments One of the authors Prof. J. Jayabharathi is thankful to DST [No. SR/S1/IC-73/2010], DRDO (NRB-213/MAT/10-11), UGC (F. No. 36-21/2008 (SR)) and CSIR (NO 3732/NS-EMRII) for providing funds to this research study.

References

1. Hush NS (1985) Distance dependence of electron transfer rates. Coord Chem Rev 64:135–157
2. Marcus RA (1989) Relation between charge transfer absorption and fluorescence spectra and the inverted region. J Phys Chem 93:3078–3086
3. Gould IR, Young RH, Moody RE, Farid S (1991) Contact and solvent-separated geminate radical ion pairs in electron-transfer photochemistry. J Phys Chem 95:2068–2080
4. Gould IR, Noukakis D, Gomez-Jahn L, Young RH, Goodman JL, Farid S (1993) Radiative and nonradiative electron transfer in contact radical-ion pairs. J Chem Phys 176:439–456
5. Cortes J, Heitele H, Jortner J (1994) Bandshape analysis of the charge transfer fluorescence in barrelene based electron-donor-acceptor compounds. J Phys Chem 98:2527–2536
6. Mulliken RS, Person WB (1969) molecular complexes: a lecture and reprint volume. VCH, Weinheim
7. Murrell JN (1959) Molecular complexes and their spectra. ix the relationship between the stability of a complex and the intensity of its charge-transfer bands. J Am Chem Soc 81:5037–5043
8. Bixon M, Jortner J, Verhoeven JW (1994) Lifetimes for radiative charge recombination in donor-acceptor molecules. J Am Chem Soc 116:7349–7355
9. Herbich J, Kapturkiewicz A (1998) Electronic structure and molecular conformation in the excited charge transfer singlet states of p-acridyl and other aryl derivatives of aromatic amines. J Am Chem Soc 120:1014–1029
10. Kapturkiewicz A, Herbich J, Karpiuk J, Nowacki J (1997) Intramolecular radiative and radiationless charge recombinations in donor-acceptor carbazole derivatives. J Phys Chem A 101:2332–2344
11. Kapturkiewicz A, Nowacki J (1999) Properties of the intramolecular excited charge-transfer states of carbazol-9-yl derivatives of aromatic ketones. J Phys Chem A 103:8145–8155
12. Borowicz P, Herbich J, Kapturkiewicz A, Nowacki J (1999) Excited charge-transfer states in donor-acceptor indole derivatives. Chem Phys 244:251–261 [13]
13. Borowicz P, Herbich J, Kapturkiewicz A, Nowacki J, Opallo M (1999) Radiative and nonradiative electron transfer in donor-acceptor phenoxazine and phenothiazine derivatives. Chem Phys 249:49–62
14. Grabowski ZR, Rotkiewicz K, Siemiarczuk A, Cow-ley DJ, Baumann W (1979) Twisted intramolecular charge transfer states (TICT). A new class of excited states with a full charge separation. Nouv J Chim 3:443–454
15. Masaki S, Okada T, Mataga N, Sakata Y, Misumi S (1976) On the solvent-induced changes of electronic structures of intramolecular exciplexes. Bull Chem Soc Jpn 49:1277–1283
16. Richard JP, Amyes TL (2001) Proton transfer at carbon. Curr Opin Chem Biol 5:626–633
17. Stoner-Ma D, Jaye AA, Ronayne KL, Nappa J, Meech SR, Tonge PJ (2008) An alternate proton acceptor for excited state protein transfer in green fluorescent protein: rewiring GFP. J Am Chem Soc 130:1227–1235
18. Paterson MJ, Robb MA, Blancafort L, DeBellis AD (2005) Mechanism of an exceptional class of photostabilizers: a seam of conical intersection parallel to excited state intramolecular proton transfer (ESIPT) in o-Hydroxyphenyl-(1,3,5)-triazine. J Phys Chem A 109:7527–7537
19. Lim SJ, Seo J, Park SY (2006) Photochromic switching of excited-state intramolecular proton-transfer (ESIPT) fluorescence: a unique route to high-contrast memory switching and nondestructive readout. J Am Chem Soc 128:14542–14547
20. Klymchenko AS, Shvadchak VV, Yuschenko DA, Jain N, Mély Y (2008) Excited-state intramolecular proton transfer distinguishes microenvironments in single- and double-stranded DNA. J Phys Chem B 112:12050–12055
21. Kwon JE, Park SY (2011) Advanced organic optoelectronic materials: harnessing excited-state intramolecular proton transfer (ESIPT) process. Adv Mater 23:3615–3642
22. Jayabharathi J, Thanikachalam V, Sathishkumar R (2012) Characterization, physiochemical and computational studies of the newly synthesized novel imidazole derivative. Spectrochim Acta Part A 97:582–588
23. Jayabharathi J, Thanikachalam V, Jayamoorthy K (2012) Computational studies of 1,2-disubstituted benzimidazole derivatives. Spectrochim Acta Part A 97:131–136, Spectrochim. Acta Part A: 93 (2012) 240–244
24. Jayabharathi J, Thanikachalam V, Brindha Devi K, Venkatesh Perumal M (2012) Kamlet-Taft and catalan studies of some novel Y-shaped imidazole derivatives. J Fluoresc 22:737–744
25. Kamlet MJ, Abboud JLM, Abraham MH, Taft RW (1983) Linear solvation energy relationships. 23. a comprehensive collection of the solvatochromic parameters, π^*, α, and β, and some methods for simplifying the generalized solvatochromic equation. J Org Chem 48:2877–2887
26. Frisch MJ, Trucks GW, Schlegel HB, Scuseria GE, Robb MA, Cheeseman JR, Montgomery JA Jr, Vreven T, Kudin KN, Burant JC, Millam JM, Iyengar SS, Tomasi J, Barone V, Mennucci B, Cossi M, Scalmani G, Rega N, Petersson GA, Nakatsuji H, Hada M, Ehara M, Toyota K, Fukuda R, Hasegawa J, Ishida M, Nakajima T, Honda Y, Kitao O, Nakai H, Klene M, Li X, Knox JE, Hratchian HP, Cross JB, Bakken V, Adamo C, Jaramillo J, Gomperts R, Stratmann RE, Yazyev O, Austin AJ, Cammi R, Pomelli C, Ochterski JW, Ayala PY, Morokuma K, Voth GA, Salvador P, Dannenberg JJ, Zakrzewski VG, Dapprich S, Daniels AD, Strain MC, Farkas O, Malick DK, Rabuck AD, Raghavachari K, Foresman JB, Ortiz JV, Cui Q, Baboul AG, Clifford S, Cioslowski J, Stefanov BB, Liu G, Liashenko A, Piskorz P, Komaromi I, Martin RL, Fox DJ, Keith T, Al-Laham MA, Peng CY, Nanayakkara A, Challacombe M, Gill PMW, Johnson B, Chen W, Wong MW, Gonzalez C, Pople JA (2004) Gaussian 03 (revision E.01). Gaussian, Inc, Wallingford
27. Skonieczny K, Ciuciu AI, Nichols EM, Hugues V, Desce MB, Flamigni L, Gryko DT (2012) Bright emission tunable fluorescent dyes based on imidazole and π- expanded imidazole. J Mater Chem 22:20649
28. Herbich J, Waluk J (1994) Excited charge transfer states in 4-amino-pyrimidines, 4-(dimethylamino)pyrimidine and 4-(dimethylamino)pyridine. Chem Phys 188:247–265
29. Jayabharathi J, Thanikachalam V, Kalaiarasi V, Jayamoorthy K (2014) Optical properties of 1-(4,5-diphenyl-1-p-tolyl-1H-imidazol-

2-yl) naphthalen-2-ol – ESIPT process. Spectrochim Acta A Mol Biomol Spectrosc 120:389–394
30. Sowmiya M, Tiwari AK, Sonu, Saha SK (2011) Study on intramolecular charge transfer fluorescence properties of trans-4-[4_-(N,N_-dimethylamino)styryl]pyridine: Effect of solvent and pH. J Photochem Photobiol Chem A 218:76–86
31. Mishina S, Takayanagi M, Nakata M, Otsuki J, Araki K (2001) Dual fluorescence of 4-dimethylaminopyridine and its derivatives: effects of methyl substitution at the pyridine ring. J Photochem Photobiol Chem A 141:153–158
32. Dubroca CC, Nouchi G, Ben Brahim M, Pesquer M, Gorse D, Cazeau P (1994) Dual fluorescence of 4-*N,N*-dimethylaminopyridine. Role of hydrogen-bonded complex in the ground state. J Photochem Photobiol Chem A 80:125–133
33. Marcus RA (1956) Electrostatic free energy and other properties of states having nonequilibrium polararization I. J Chem Phys 24:966–979
34. McGlynn SP, Azumi T, Kinoshita M (1969) Molecular spectroscopy of the triplet state. Prentice Hall, Englewood Cliffs, NJ
35. Willard DM, Riter RE, Levinger NE (1998) Dynamics of polar solvation in lecithin/water/cyclohexane reverse micelles. J Am Chem Soc 120:4151–4160
36. Saha S, Samanta A (2002) Influence of the structure of the amino group and polarity of the medium on the photophysical behavior of 4-amino-1,8-naphthalimide derivatives. J Phys Chem A 106:4763
37. Reichardt C (1988) Solvents and solvent effects in organic chemistry, 2nd edn. VCH, Weinheim
38. Lippert E (1957) Spektroskopische bistimmung des dipolmomentes aromatischer verbindugen imersten angeregten singulettzustand. Z Electrochem 61:962–975
39. Reichardt C (1979) Empirical parameters of solvent polarity as linear free energy relationships. Angew Chem Int Ed Engl 18:98–110
40. Haidekker MA, Brady TP, Lichlyter D, Theodorakis EA (2005) Effects of solvent polarity and solvent viscosity on the fluorescent properties of molecular rotors and related probes. Bioorg Chem 33: 415–425
41. Rettig W, Zander M (1982) On twisted intramolecular charge transfer (TICT) stated in N-aryl-carbazoles. Chem Phys Lett 87:229–234
42. Allinger NL (1976) Ground state geometry optimizations were done using MMX force field, PCMODEL from Serena Software. Adv Phys Org Chem 13:1
43. Bo¨ttcher CJF (1973) Theory of electric polarization. Elsevier: Amsterdam, 1952, 2nd edn. Revised by Van Belle OC, Bordewijk P, Rip A, Vol. 1 and 2. Elsevier: Amsterdam
44. Birks JB (1970) Photophysics of aromatic molecules. Wiley, New York, p 51
45. Mataga N, Kaifu Y, Koizumi M (1955) The Solvent Effect on Fluorescence Spectrum. Change of Solute-Solvent Interaction During the Lifetime of Excited Solute Molecule. Bull Chem Soc Jpn 28:690–691
46. Liptay W, Lim EC (eds) (1974) In excited state. Academic Press, New York, p 129
47. Grabowski ZR, Dobkowski J (1983) Twisted intramolecular charge transfer (TICT) excited states: energy and molecular structure. Pure Appl Chem 55:245–252
48. Hotchandani S, Testa AC (1973) Phosphorescence emission and polarization of aminopyridines. J Chem Phys 59:596–600
49. Babiak S, Testa AC (1976) Fluorescence lifetime study of aminopyridines. J Phys Chem 80:1882–1885
50. Birks JB (1978) Photophysics of aromatic molecules. Wiley, New York
51. Michl J, Thulstrup EW (1986) Spectroscopy with polarized light. Wiley, New York
52. Mulliken RS (1952) Molecular compounds and their spectra. J Am Chem Soc 74:811–824
53. Mulliken RS, Person WB (1969) Molecular complexes: a lecture and reprint volume. Wiley, New York
54. Herbich J, Kapturkiewicz A, Nowacki J, Golinski J, Dabrowski Z (2001) Intramolecular excited charge-transfer states in donor-acceptor derivatives of naphthalene and azanaphthalenes. Phys Chem Chem Phys 3:2438–2449
55. Innes KK, Ross IG, Moomaw WR (1988) Electronic states of azabenzenes and azanaphthalenes: a revised and extended critical review J. Mol Spectrosc 132:492–544
56. Castellan A, Michl J (1978) Magnetic circular dichroism of cyclic.pi.-electron systems. 4. Aza analogs of benzene. J Am Chem Soc 100:6824–6827
57. Dogonadze RR, Kuznetsov AM, Marsagishvili T (1980) The present state of the theory of charge transfer in condensed phase. Electrochim Acta 25:1–28
58. Heicrbh J, Grabowski ZR, Wojtowicz H, Golankiewicz K (1989) Dual fluorescence of 4-(dialkilamino)pyrimidines. Twisted charge transfer state formation favored by hydrogen bond or by coordination to the metal ion. J Phys Chem 93: 3439–3444
59. Marcus RA (1963) Free energy of nonequilibrium polarization systems. II. Homogeneous and electrode systems. J Chem Phys 38: 1858–1862
60. Castellan GW (1985) Physical chemistry, 3rd edn. Narosa Publishing House, Delhi
61. Kapturkiewicz A (1992) Electrochemical generation of excited TICT states. V. Evidence of inverted Marcus region. Chem Phy 166:259–273
62. Turro NJ, Ramamurthy V, Scaiano JC (2009) Principles of molecular photochemistry, Chapter 7.37. University Science Books, Sausalito